Slowing Down of Accelerated Structural Relaxation in Ultrathin Polymer Films

Qiyun Tang* and Wenbing Hu†
Department of Polymer Science and Engineering, State Key Laboratory of Coordination Chemistry, School of Chemistry and Chemical Engineering, Nanjing University, 210093 Nanjing, China

Simone Napolitano
Laboratory of Polymer and Soft Matter Dynamics, Faculté des Sciences, Université Libre de Bruxelles (ULB), Boulevard du Triomphe, Bâtiment NO, Bruxelles 1050, Belgium

(Received 8 November 2013; published 10 April 2014)

We demonstrate with molecular simulation that the acceleration of structural relaxation, also known as physical aging, commonly experimentally observed in thin polymer films slows down at extremely small thicknesses. This phenomenon can be attributed to an inversed free volume diffusion process caused by the sliding motion of chain molecules. Our findings provide direct evidence of the relationship between the sliding motion of short chain fragments and the structural relaxation of ultrathin polymer films, and also verify the existence of a new confinement effect at the nanoscale.

DOI: 10.1103/PhysRevLett.112.148306 PACS numbers: 82.35.Lr, 73.50.-h, 76.60.-k, 81.40.Cd

The investigation of structural relaxation of polymers in the glassy state, often referred to as physical aging, has attracted continuous attention in the last decades, due to the strong influence of these phenomena on the performance and lifetime of polymer-based devices [1–5]. Several experiments demonstrated that, upon confinement at the nanoscale level, the physical aging rate [6–14] was enhanced in comparison to the bulk. For example, measurements performed on freestanding films showed a pronounced reduction in gas permeability [10] and faster enthalpy recovery [14], indicating an acceleration in the physical aging upon the reduction of film thickness. This peculiar behavior could be reproduced by the free volume holes diffusion model [15–18], on the basis of the larger contribution of surface mobile layers upon reduction of the film thickness. Free surfaces, in fact, increase the average segmental mobility of the entire thin films, which yields a larger diffusion of free volume holes towards the surface. The occurrence of this phenomenon accelerates physical aging and, thus, reduces the lifetime and potential application of polymer-based nanodevices [4].

The molecular mechanisms governing the dynamics of confined systems are still not clear [19]. Recent experimental evidences suggest that the glassy-state structural relaxation is affected by local segmental motions [20]. For example, Chowdhury *et al.* [20] found that the rearrangements of a few number of segments were sufficient to relax local chain conformations and that this process would be responsible for macroscopic relaxations near the surface. Frieberg *et al.* showed that films of star-shaped polymers relax slower than those of linear macromolecules [21] and that the aging rate is particularly sensitive to both the functionality and the arm length [22]. The possible molecular origin of this anomalous behavior might be attributed to the suppression of sliding motions between "kinks" (proposed by de Gennes [23–25] and extended by Milner *et al.* [26,27]) along the contour of the chain by the existence of core points (grafting points) in star-shaped polymers [28]. This indicates that the motions of short chain fragments would strongly influence the relaxation of the entire polymer films.

Here, we demonstrate with molecular simulation that the acceleration in physical aging commonly observed experimentally in thin films of linear polymers is strongly reduced at extremely small thicknesses. We also show that the onset thickness shifts to lower value in the case of low molecular-weight compounds. This abnormal behavior can be attributed to the occurrence of an inversed free volume diffusion process caused by the sliding motion [23–25] of chain molecules between the two free surfaces. Our results provide direct evidence of the relationship between the motion of short chain fragments and the structural relaxation of ultrathin polymer films. More interestingly, we verify that the average length of short chain fragments defines a critical film thickness and demonstrate the existence of a new confinement effect.

In this Letter, we employ our recently developed simulation methods [29] to investigate in detail the influence of film thickness on the structural relaxation of ultrathin polymer films. In our simulation, the vacancies represent the "excess" free volume holes in films and the air molecules have repulsive interaction with chain segments to form two smooth free surface layers [see Fig. 1(a) and Supplemental Material [30]]. Figure 1(b) shows the typical time evolution [31] of the reduced volume $V(t)/V(0)$ for a film of thickness $H = 8$ at the temperature $T = 4.8$. Here, $V(t)$ and $V(0)$ represent the volumes of the film at time t and reference time $t = 0$. The relaxation rate can be associated to the slope of $V(t)/V(0)$ as a function of the logarithm of the time [13,29,32]:

$$\beta = -\frac{1}{V_0}\frac{dV(t)}{d\log t} = -\frac{d[V(t)/V_0]}{d\log t}, \quad (1)$$

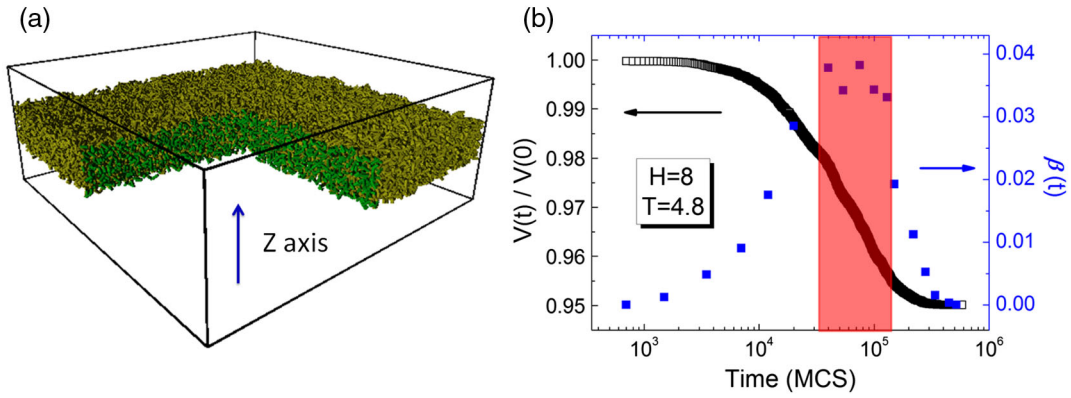

FIG. 1 (color online). (a) Snapshot of the freestanding ultrathin polymer film. (b) Time evolution of the reduced volume $V(t)/V(0)$ and the corresponding relaxation rate $\beta(t)$ of ultrathin film with thickness $H = 8$ at temperature $T = 4.8$.

where $V_0 = V(0)$. Figure 1(b) also illustrates the variation of the corresponding relaxation rate $\beta(t)$ as a function of time. It is depicted that $\beta(t)$ shows a peak in the relaxation region [shaded area in Fig. 1(b)]. In the following, we employ the mean value of $\beta(t)$ in this region to represent the relaxation rate of ultrathin films.

Figure 2(a) shows the thickness dependence of the relaxation rate in films with chain length of $N = 400$ and the same initial free volume concentration $\phi_{v0} = 0.05$. Each point was obtained by averaging the relaxation rates extracted from six independent simulations. As the film thickness decreases towards $H = 9$, the relaxation rate gradually increases, which is consistent with experiments [10,14]. This indicates that our model could reproduce the accelerated physical aging in thin polymer films [6–14]. More importantly, the outlined simulations could access the detailed information of volume relaxation in extremely thin films, where the relaxation time scales are too short to be experimentally assessed at the state of the art [10,14] (see discussions in the Supplemental Material [30]). Remarkably, upon further reduction of the thickness, such as at $H = 6$, the relaxation rate drops down. At the best of our knowledge, there is no evidence from experiments or simulations showing a slowing down of the acceleration in physical aging in freestanding ultrathin polymer films. Here, it should be noted that during the experimental preparation of ultrathin polymer films, the initial free volume concentration ϕ_{v0} would greatly vary at different H. Previously, we showed that the magnitude of ϕ_{v0} just added a factor on the aging rate of ultrathin polymer films [29]. In this case, experimental aging rate normalized by the measured ϕ_{v0}, could be compared to our simulation results.

The emergence of a peak in the thickness dependence of β indicates the existence of two competing mechanisms that contribute to the relaxation rate. In our previous work [29], we demonstrated that the average segmental mobility and the accurate initial free volume concentration ϕ_{vi} distinctly influence $\beta(H)$. The instantaneous segmental mobility in ultrathin films can be computed as [29,33,34]:

$$\alpha(t) = 1 - \sum_{i=1}^{n}\sum_{j=1}^{N} \delta[\boldsymbol{r}_{ij}(t) - \boldsymbol{r}_{ij}(t - \Delta t)]/N_{\text{total}}, \qquad (2)$$

where $\boldsymbol{r}_{ij}(t)$ represents the position of segment j in the i-th chain at the t-th MC step, N_{total} is the total number of segments, and $\Delta t = 1$ MC step. The average segment mobility α is obtained by averaging $\alpha(t)$ when the films approaching equilibrium state [29]. The layered $\alpha(z)$ is calculated by using $\alpha(z) = \alpha\delta(z)$, see inset in Fig. 3(a), where the $\alpha(z)$ near the surface layer is higher than that in the core of the film, similar to other simulations [35–39] and experiments [40]. Upon reduction of the thickness, the portion of the surface mobile layers increases, leading to a larger α [see Fig. 3(a)]. This accelerates the free volume diffusion and vanishing processes, enhancing the structural relaxation correspondingly. Another mechanism contributing to $\beta(H)$ is thickness dependence of the accurate initial free volume concentration ϕ_{vi} [41] [inset in Fig. 3(b)]. Figure 3(b) shows that, as the thickness decreases, ϕ_{vi} declines correspondingly. This reduction can be attributed to the enhanced reduction of reduced volume within the initial plateau at larger segmental mobility [see Fig. 3(a)]. This parameter has a similar temperature dependence as that of ϕ_{vi} [29]. Thus, decreasing film thickness corresponds to a reduction of ϕ_{vi}, which lowers the relaxation rate. Combining the two mechanisms, we can qualitatively conclude that, upon confinement, $\beta(H)$ drops after crossing a maximum at a critical film thickness. Consequently, the accelerated structural relaxation observed in ultrathin polymer films would eventually be suppressed at extremely small thicknesses.

Understanding the origin of this phenomenon would be very useful for the design of polymer-based nanodevices. The appearance of a peak in $\beta(H)$ indicates, in fact, the existence of a thickness regime with improved lifetime. To explore the universality of this phenomenon, we evaluated the thickness dependence of the relaxation rate in ultrathin films with two other chain lengths, $N = 100$ and 5, shown in Figs. 2(b) and 2(c), respectively (simulation details for $N = 5$ can be found in Supplemental Material [30]). For $N = 100$, the drop in $\beta(H)$ is still present and onsets at nearly the same thickness $H = 6$, while for $N = 5$, the onset thickness shifts to lower value of $H = 5$. This behavior indicates that the slowing down of accelerated relaxation strongly depends on the size of chain molecules. As a first attempt, we normalized the film thickness by the radius of gyration (R_g) (see Fig. S4). As this procedure

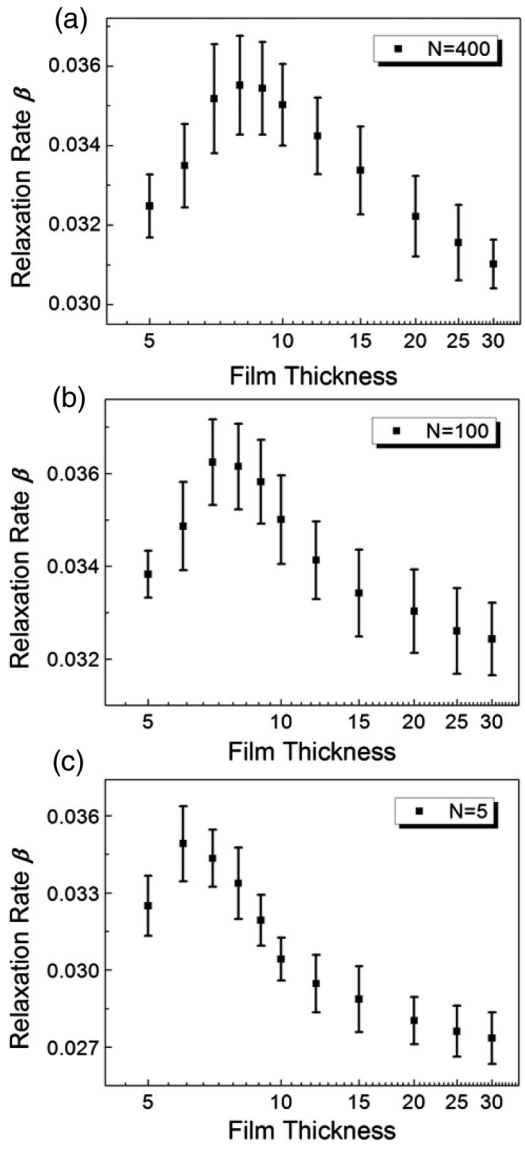

FIG. 2. Thickness dependence of relaxation rate β in ultrathin polymer films at temperature $T = 4.8$. The films are constructed by polymers with chain length of (a) $N = 400$, (b) $N = 100$, and (c) $N = 5$.

failed in providing a master curve of $\beta(H/R_g)$, the size of the random coil does not represent the critical dimension that could account for the slowing down of accelerated relaxations observed in Fig. 2. In the next paragraphs, we provide an analysis of this phenomenon permitting to identify an appropriate molecular length scale for the abnormal relaxation behavior of polymer films.

Due to the nonreversible free volume vanishing process occurring at the two free surfaces [29], the free volume holes within polymer films normally tend to diffuse from the core towards the two surface regions. This diffusion determines the aging rate of quenched polymer films. However, at extremely small thicknesses, an inversed free volume diffusion (IFVD) becomes relevant. Inset in Fig. 4(a) illustrates the IFVD mechanism, where a successful jump of segment B into a free volume hole C draws

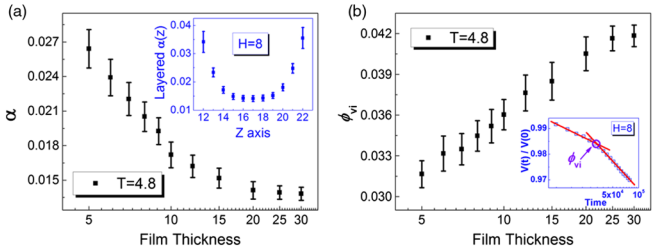

FIG. 3 (color online). (a) Thickness dependence of the average segment mobility α in ultrathin films with chain length $N = 400$. Inset shows the layered $\alpha(z)$ within the film (stays from 12 to 22 on the Z axis) with thickness $H = 8$. (b) Variation of the accurate initial free volume concentration ϕ_{vi} as a function of film thickness. Inset illustrates the intersection point that defines the ϕ_{vi}.

the chain along its contour direction until approaching the position of a kink segment A, which diffuses free volume hole C into the position of segment A. Here, the kink segments A and B are located at the upper and lower surface layers correspondingly; thus, they take nearly the same mobilities and energies. In this case, the movements of segments A or B will diffuse the free volume hole C back and forth between the two surfaces without introducing additional energetic cost (see Supplemental Material [30]), giving rise to the IFVD process. The slithering diffusion terminated by extending the nearest kink conformation along the chain was reported [42] with a combination of a kink-jump method and the "slithering snake" ("reptation") algorithms [43]. This procedure provided a direct evidence of the sliding motion proposed by de Gennes [23–25] and was recognized as a powerful technique in the simulation of polymer systems [44]. Additionally, the occurrence of sliding motion in ultrathin polymer films had already been verified recently by experiments [45], in which the surface patterning of polystyrene films could be remotely controlled by altering the nature of the substrate. To get a deeper insight on the IFVD mechanism, we counted the number of free volume holes diffused inversely between the lower and upper surface regions, $N_{IFVD}(t, \Delta t)$ with $\Delta t = 10$ MCS, and calculated the inversed diffusion rate:

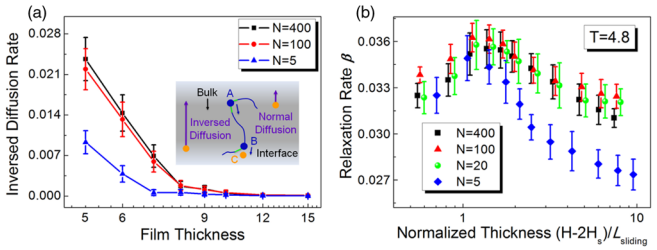

FIG. 4 (color online). (a) Thickness dependence of inversed free volume diffusion rate in ultrathin films. Inset illustrates the IFVD process caused by the sliding motion along chain molecules. (b) Variation of relaxation rate as a function of normalized film thickness $(H - 2H_s)/L_{\text{sliding}}$.

$$\gamma(t) = \frac{N_{IFVD}(t, \Delta t)}{N_f(t)}, \quad (3)$$

where $N_f(t)$ is the number of free volume holes at time t [46]. Figure 4(a) shows the variation of the average value of $\gamma(t)$ as a function of film thickness for different N. The inversed diffusion rate for $N = 400$ and $N = 100$ increases gradually when the film thickness approaches extremely small values (such as $H <= 9$). This behavior indicates that, upon reduction of the thickness, the IFVD between the two surfaces gradually becomes predominant, and on average, hinders the normal diffusion of free volume holes and their consecutive vanishing at the free surfaces, resulting in the slowing down of accelerated structural relaxation at extremely small thickness [see Figs. 2(a) and 2(b)].

Based on the definition of inversed free volume diffusion, we can expect that the IFVD becomes relevant when the portion of the film not occupied by surfaces is smaller than the average sliding length between the nearest kink segments A and B along one chain [44], L_{sliding} [see the inset in Fig. 4(a)], that is, $H - 2H_s < L_{\text{sliding}}$, where H_s indicates the thickness of the surface layer. To prove this hypothesis, we calculated L_{sliding} as a function of N [47,48] (see Supplemental Material [30]) and compared the IFVD rate for films of the same H, but different N. In our simulation, L_{sliding} holds the average values of 3.6 and 3.5 for $N = 400$ and 100, and 2.8 for $N = 5$ (see Fig. S6). At $H = 6$, $H - 2H_s$ takes the same value of 3, regardless of N [49], which is smaller than L_{sliding} for $N = 400$ and 100, but larger than that for $N = 5$. Thus, at $H = 6$ the IFVD is predominant for films with $N = 400$ and $N = 100$ [the average $\gamma(t)$ takes the value of about 0.014], while for $N = 5$, the inversed diffusion is not relevant [average $\gamma(t) \simeq 0.004$]. These findings are consistent with our hypothesis. Plotting the relaxation rates at different N, as a function of the thickness of the bulk layer normalized by the average sliding length, permitted to collapse the different curves over the same maximum, at $(H - 2H_s)/L_{\text{sliding}} \simeq 1.0$ [see Fig. 4(b), β for $N = 20$ are calculated for comparison, and the deviations of β for $N = 5$ at thicker thicknesses are discussed in Supplemental Material [30]]. Our findings demonstrate the significance of the sliding motion of short chain fragments on the slowing down of accelerated structural relaxation in ultrathin polymer films. We speculate that such behavior would not exist for simple molecules ($N = 1$), where the sliding motion does not occur, in line with the idea of de Gennes [24].

The critical thickness defined by $H_c = L_{\text{sliding}}(N) + 2H_s$ indicates a new length scale of confinement. Finite size effects emerge when the thickness of polymer films approaches few folds R_g. In this thickness regime, the conformational entropy greatly varies due to the compression of chains along the confinement direction, which results in the change of physical properties as a function of the thickness [24,25,45]. Our findings demonstrate that the relaxation rate of ultrathin polymer films is perturbed when the thickness approaches another critical length defined by H_c. As shown in Fig. S6, it can be concluded that, for long enough chains, H_c is far lower than R_g. This indicates that a new confinement effect appears in ultrathin films at thicknesses comparable to H_c. The real length of H_c could be roughly estimated for polystyrene [55] (see Supplemental Material [30]), which takes the value of 6.6 nm for $N = 400$. More importantly, this new confinement effect would probably not exist in films of simple molecules, which means that chain connectivity dominates the relaxation behaviors at the nanoscale [56]. These findings shed light on the possibility of unveiling the molecular origins of the abnormal behavior of ultrastable polymer glasses [57] compared to that of low molecular weight glasses [58,59] and liquids with enhanced orientational order [60].

In conclusion, we demonstrate that the accelerated structural relaxation in freestanding polymer films is suppressed when the system is confined at extremely small thicknesses. The observed anomalous phenomenon is attributed to the inversed free volume diffusion process caused by the sliding motion of chain molecules. Our results provide direct evidence for the relationship between the sliding motions of short chain fragments and the structural relaxation of ultrathin polymer films. We also identify the existence of a new confinement effect at the nanoscale. The outlined approach, here exploited in the case of linear chain, could be easily extended to polymers with more complex architectures [21,22] and unveil the correlations between the structure and dynamics in ultrathin polymer films.

We acknowledge the helpful discussions from Professor Günter Reiter, Professor Jens-Uwe Sommer, Dr. Daniele Cangialosi, and Professor Rodney Priestley. This work was supported by National Natural Science Foundation of China (Grants No. 20825415 and No. 21274061), National Basic Research Program of China (Grant No. 2011CB606100), China Postdoctoral Science Foundation (Grant No. 2013M531319), Program for Changjiang Scholars and Innovative Research Team in University, and the FER funds of the Université Libre de Bruxelles.

*tqy553new@gmail.com
†wbhu@nju.edu.cn

[1] L. C. E. Struik, *Physical Aging in Amorphous Polymers and Other Materials* (Elsevier, Amsterdam, 1978).
[2] I. M. Hodge, Science **267**, 1945 (1995).
[3] J. M. Hutchinson, Prog. Polym. Sci. **20**, 703 (1995).
[4] R. D. Priestley, Soft Matter **5**, 919 (2009).
[5] D. Cangialosi, V. M. Boucher, A. Alegria, and J. Colmenero, Phys. Rev. Lett. **111**, 095701 (2013).
[6] P. H. Pfromm and W. J. Koros, Polymer **36**, 2379 (1995).
[7] K. D. Dorkenoo and P. H. Pfromm, Macromolecules **33**, 3747 (2000).
[8] M. S. McCaig and D. R. Paul, Polymer **41**, 629 (2000).
[9] D. Cangialosi, M. Wübbenhorst, J. Groenewold, E. Mendes, H. Schut, A. van Veen, and S. J. Picken, Phys. Rev. B **70**, 224213 (2004).

[10] Y. Huang and D. R. Paul, Polymer **45**, 8377 (2004).
[11] C. Zhou, T.-S. Chung, R. Wang, and S. H. Goh, J. Appl. Polym. Sci. **92**, 1758 (2004).
[12] Y. Huang and D. R. Paul, Macromolecules **38**, 10148 (2005).
[13] R. D. Priestley, C. J. Ellison, L. J. Broadbelt, and J. M. Torkelson, Science **309**, 456 (2005).
[14] V. M. Boucher, D. Cangialosi, A. Alegria, and J. Colmenero, Macromolecules **45**, 5296 (2012).
[15] T. Alfrey, G. Goldfinger, and H. Mark, J. Appl. Phys. **14**, 700 (1943).
[16] J. G. Curro, R. R. Lagasse, and R. Simha, Macromolecules **15**, 1621 (1982).
[17] D. Cangialosi, V. M. Boucher, A. Alegria, and J. Colmenero, J. Chem. Phys. **135**, 014901 (2011).
[18] S. Napolitano and D. Cangialosi, Macromolecules **46**, 8051 (2013).
[19] S. Napolitano, S. Capponi, and B. Vanroy, Eur. Phys. J. E **36**, 61 (2013).
[20] M. Chowdhury, P. Freyberg, F. Ziebert, Arnold C.-M. Yang, U. Steiner, and G. Reiter, Phys. Rev. Lett. **109**, 136102 (2012).
[21] B. Frieberg, E. Glynos, G. Sakellariou, and P. F. Green, ACS Macro Lett. **1**, 636 (2012).
[22] B. Frieberg, E. Glynos, and P. F. Green, Phys. Rev. Lett. **108**, 268304 (2012).
[23] P. G. de Gennes, J. Chem. Phys. **55**, 572 (1971).
[24] P. G. de Gennes, Eur. Phys. J. E **2**, 201 (2000).
[25] P. G. de Gennes, C. R. Acad. Sci. Ser. Gen., Ser. 4 **1**, 1179 (2000).
[26] S. T. Milner and J. E. G. Lipson, Macromolecules **43**, 9865 (2010).
[27] J. E. G. Lipson and S. T. Milner, Macromolecules **43**, 9874 (2010).
[28] E. Glynos, B. Frieberg, H. Oh, M. Liu, D. W. Gidley, and P. F. Green, Phys. Rev. Lett. **106**, 128301 (2011).
[29] Q. Tang and W. Hu, Phys. Chem. Chem. Phys. **15**, 20679 (2013).
[30] See Supplemental Material at http://link.aps.org/supplemental/10.1103/PhysRevLett.112.148306 for simulation details and additional discussion.
[31] The unit of time evolution is defined as one Monte Carlo step (MCS), including the number of trial moves equal to the number of segments in the sample system.
[32] E. A. Baker, P. Rittigstein, J. M. Torkelson, and C. B. Roth, J. Polym. Sci. B **47**, 2509 (2009).
[33] C. Bennemann, C. Donati, J. Baschnagel, and S. C. Glotzer, Nature (London) **399**, 246 (1999).
[34] A. R. C. Baljon, J. Billen, and R. Khare, Phys. Rev. Lett. **93**, 255701 (2004).
[35] H. Morita, K. Tanaka, T. Kajiyama, T. Nishi, and M. Doi, Macromolecules **39**, 6233 (2006).
[36] S. Peter, H. Meyer, and J. Baschnagel, J. Polym. Sci. Polym. Phys. Ed. **44**, 2951 (2006).
[37] S. Peter, S. Napolitano, H. Meyer, M. Wübbenhorst, and J. Baschnagel, Macromolecules **41**, 7729 (2008).
[38] C. Batistakis, A. V. Lyulin, and M. A. J. Michels, Macromolecules **45**, 7282 (2012).
[39] C. Batistakis, M. A. J. Michels, and A. V. Lyulin, J. Chem. Phys. **139**, 024906 (2013).
[40] S. Kim and J. M. Torkelson, Macromolecules **44**, 4546 (2011).
[41] ϕ_{vi} is defined by the intersection point of the initial plateau and the linear relaxation region on the reduced volume curve, see inset in Fig. 3(b). Here, the two straight lines are the best fits of the reduced volume in the two regimes and the number of free volume holes at the intersection point is $N_v^*(t) = V^*(t) - \mathcal{N}$, with $\mathcal{N}$ the number of segments in the film and $V^*(t)$ is the volume of film at the intersection point. Thus, ϕ_{vi} is obtained by $\phi_{vi} = N_v^*(t)/[nN + N_v^*(t)]$. As shown in our previous paper [29], ϕ_{vi} represents the deviations of quenched polymer films from equilibrium states, similar to the qualitative description of the deviations by $\Delta T = T_a - T_g$ in experiments, where T_a is the aging temperature.
[42] W. Hu, J. Chem. Phys. **109**, 3686 (1998).
[43] K. Kremer and K. Binder, Comput. Phys. Rep. **7**, 259 (1988).
[44] W. Hu and D. Frenkel, Adv. Polym. Sci. **191**, 1 (2005).
[45] I. Siretanu, J. P. Chapel, and C. Drummond, Macromolecules **45**, 1001 (2012).
[46] Δt evaluated at different values shows similar relationship of the inversed diffusion rate at distinct film thicknesses. Detailed discussion about the time evolution of $\gamma(t)$ for distinct H is given in the Supplemental Material [30].
[47] M. Lang and J. U. Sommer, Phys. Rev. Lett. **104**, 177801 (2010).
[48] The average sliding length L_{sliding} is calculated from the length l_{AB} between kink segments A and B from our simulation data. See [44] for details. We should note that in [47], the calculated entanglement length (similar to l_{AB}) is nearly 11. In our simulation, l_{AB} could also approach 11, but with low probability. Most values of l_{AB} are accumulated within the range from 2 to 5.
[49] Here, H_s only depends on the attractive nonbonded segment-segment interaction (see Fig. S3 and the discussions in Supplemental Material [30], which includes Refs. [50–54]). From Fig. S3(b), the bulk region for the film with $H = 6$ occupies a thickness $H_{\text{bulk}} = 3$; thus, we obtain $2H_s = H - H_{\text{bulk}} = 3$. We have verified that $2H_s$ is thickness independent.
[50] A. J. Kovacs, Adv. Polym. Sci. **3**, 394 (1963).
[51] S. Napolitano, C. Rotella, and M. Wubbenhorst, ACS Macro Lett. **1**, 1189 (2012).
[52] Y. P. Koh and S. L. Simon, J. Polym. Sci. B **46**, 2741 (2008).
[53] M. L. Williams, R. F. Landel, and J. D. Ferry, J. Am. Chem. Soc. **77**, 3701 (1955).
[54] J. Brandrup, E. H. Immergut, and E. A. Grulke, *Polymer Handbook* (John Wiley & Sons, New York, 2003), fourth ed.
[55] G. D. Wignall, J. Schelten, and D. G. H. Ballard, J. Appl. Crystallogr. **7**, 190 (1974).
[56] Here, it is worthy noting that entanglements would not affect our results because their impact should be relevant only when considering the motion of chain molecules at length scales larger than that of reptation (sliding motion) of short chain fragments [23,24], which, instead, dominates our main findings.
[57] Y. Guo, A. Morozov, D. Schneider, J. W. Chung, C. Zhang, M. Waldmann, N. Yao, G. Fytas, C. B. Arnold, and R. D. Priestley, Nat. Mater. **11**, 337 (2012).
[58] S. F. Swallen, K. L. Kearns, M. K. Mapes, Y. S. Kim, R. J. McMahon, M. D. Ediger, T. Wu, L. Yu, and S. Satija, Science **315**, 353 (2007).
[59] S. Singh, M. D. Ediger, and J. J. de Pablo, Nat. Mater. **12**, 139 (2013).
[60] S. Capponi, S. Napolitano, and M. Wubbenhorst, Nat. Commun. **3**, 1233 (2012).